Journal Pre-proofs


# Design, synthesis and biological evaluation of potent EGFR kinase inhibitors against 19D/T790M/C797S mutation

Zhicheng Su, Tingyuan Yang, Jie Wang, Mengzhen Lai, Linjiang Tong, Gulinuer Wumaier, Zhuo Chen, Shengqing Li, Honglin Li, Hua Xie, Zhenjiang Zhao

PII: S0960-894X(20)30438-8
DOI: https://doi.org/10.1016/j.bmcl.2020.127327
Reference: BMCL 127327

To appear in: *Bioorganic & Medicinal Chemistry Letters*

Received Date: 16 April 2020
Revised Date: 26 May 2020
Accepted Date: 4 June 2020

Please cite this article as: Su, Z., Yang, T., Wang, J., Lai, M., Tong, L., Wumaier, G., Chen, Z., Li, S., Li, H., Xie, H., Zhao, Z., Design, synthesis and biological evaluation of potent EGFR kinase inhibitors against 19D/T790M/C797S mutation, *Bioorganic & Medicinal Chemistry Letters* (2020), doi: https://doi.org/10.1016/j.bmcl.2020.127327

## Graphical Abstract

To create your abstract, type over the instructions in the template box below.
Fonts or abstract dimensions should not be changed or altered.

**Design, synthesis and biological evaluation of potent EGFR kinase inhibitors against 19D/T790M/C797S mutation**

A novel indole derivative **12e** was designed as a potential fourth generation EGFR$^{19D/T790M/C797S}$

Zhicheng Su[#,a] , Tingyuan Yang[#,a], Jie Wang[#,a], Mengzhen Lai[b,d], Linjiang Tong[b], Gulinuer·Wumaier[c], Zhuo Chen[a,*], Shengqing Li[c], Honglin Li[a], Hua Xie[b,*], Zhenjiang Zhao[a,*]

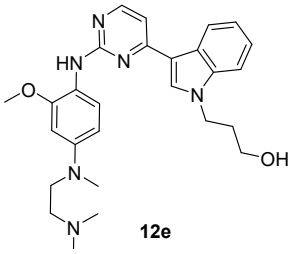


12e

| | IC50 (nM) |
|---|---|
| EGFR$^{19D/T790M/C797S}$ | 15.3 |
| EGFR $^{L858R/T790M/C797S}$ | 218.3 |
| EGFR $^{L858R/T790M}$ | 156.6 |
| EGFR $^{WT}$ | >1000 |

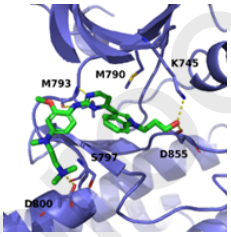

Bioorganic & Medicinal Chemistry Letters
journal homepage: www.elsevier.com

# Design, synthesis and biological evaluation of potent EGFR kinase inhibitors against 19D/T790M/C797S mutation

Zhicheng Su[#,a] , Tingyuan Yang[#,a], Jie Wang[#,a], Mengzhen Lai[b,d], Linjiang Tong[b], Gulinuer·Wumaier[c], Zhuo Chen[a,*], Shengqing Li[c], Honglin Li[a], Hua Xie[b,*], Zhenjiang Zhao[a,*]

[a] *Shanghai Key Laboratory of New Drug Design, School of Pharmacy, East China University of Science & Technology, Shanghai 200237, China*
[b] *Division of Anti-tumor Pharmacology, State Key Laboratory of Drug Research, Shanghai Institute of Materia Medica, Chinese Academy of Sciences, Shanghai 201203, China.*
[c] *Department of Pulmonary and Critical Care Medicine, Huashan Hospital, Fudan University, Shanghai, China.*
[d] *School of Pharmacy, Fudan University, Shanghai 201203, China*
[#] *Authors contributed equally to this work.*

ARTICLE INFO

*Article history:*
Received
Revised
Accepted
Available online

*Keywords:*
EGFR
NSCLC
C797S

ABSTRACT

The efficacy of EGFR inhibitors is frequently affected by acquired resistance. $EGFR^{19D/T790M/C797S}$ mutation is one of the primary reasons for the emergence of resistance after treatment with the third-generation EGFR inhibitors such as AZD9291, CO1686 and Olmutinib. To overcome the resistance mutation 19D/T790M/C797S, we designed and prepared a series of indole derivatives with the terminal hydroxyl of alkyl chain to increase extra interaction with the Asp855 in the conservative DFG site. Activity evaluation, structure-activity relationship and docking analysis were also carried out. Among them, compound **12e** displayed significant inhibitory activity against $EGFR^{19D/T790M/C797S}$ ($IC_{50}$ =15.3 nM) and good selectivity over EGFR WT ($IC_{50}$ > 1000 nM), L858R/T790M ($IC_{50}$, 156.6 nM) and L858R/T790M/C797S ($IC_{50}$, 218.3 nM) respectively. Furthermore, **12e** exhibited good growth inhibition activity, induced G1 phase cell cycle arrest and apoptosis in BaF3/$EGFR^{19D/T790M/C797S}$ cells by suppressing EGFR phosphorylation signaling pathway. In all, our study might provide a novel structural design method and lay the solid foundation for the development of the 4th generation $EGFR^{19D/T790M/C797S}$ inhibitors.



Lung cancer is the leading cause of cancer-related deaths in male or female worldwide, in which non-small cell lung cancer (NSCLC) accounts for 85% of lung cancer[1]. EGFR is a member of the ErbB receptor tyrosine family and plays a key role in cell proliferation, differentiation and apoptosis[2]. Meanwhile, EGFR mutations have an important impact on cell growth and other physiological processes. Thus, EGFR is a promising drug target in the treatment of NSCLC. First-generation EGFR inhibitors (Gefitinib and Erlotinib) show high inhibitory activity for the patients with sensitizing EGFR mutations, namely L858R mutation and exon 19 deletion[3,4]. However, acquired drug resistance occurs on patients who gain benefits from the first generation EGFR inhibitors. Approximately 60% of the acquired mutation is the $EGFR^{T790M}$ point mutation, which reduces the binding affinity towards drugs and reinforces interaction with ATP[5]. To overcome T790M resistance mutation, second-generation EGFR inhibitors (Afatinib and Dacomitinib) have been developed by introducing a Michael acceptor to form a covalent bond with Cys797 residue[6]. Nevertheless, due to the lack of selectivity between WT EGFR and mutant EGFR, the second-generation EGFR inhibitors cause serious side effects[7]. The development of third-generation EGFR inhibitors (Olmutinib and AZD9291) with aminopyrimidine as a novel scaffold successfully avoid these problems[8,9].

However, acquired resistance reappeared during the period of clinical treatment with the third-generation EGFR inhibitors such as AZD9291 and Olmutinib. At present, some studies have found that the tertiary EGFR exon 20 C797S mutation appeared to be the most common in a variety of drug resistance mechanisms. For example, Thress et al first exposed that C797S mutation was one of the causes of AZD9291 resistance[10]. Subsequently, Yu et al reported that a patient bearing $EGFR^{19D/T790M}$ mutations was detected C797S mutation after treated with AZD9291 for 9 months[11]. Meanwhile, one study also revealed that C797S mutation appeared in patients treated with Olmutinib[12]. It was the C797S mutation that disrupted the covalent bond between inhibitors and Cys797 residue and caused the loss of inhibitor activity.

*Corresponding author. Tel.: +86-21-64253962; email: zhjzhao@ecust.edu.cn, hxie@simm.ac.cn, chenzhuo@ecust.edu.cn

an emergent issue, but so far, few researches have been done. Recently, some potential EGFR inhibitors for the EGFR$^{L858R/T790M/C797S}$ mutation have been reported with high inhibitory activity[13,14,15,16]. Meanwhile, Park et al found some inhibitors against EGFR$^{19D/T790M/C797S}$ mutation by virtual screening[14]. Since previous research found that 19D/T790M/C797S mutation is more general phenomenon in patients after the use of third-generation drug AZD9291[17], we herein reported the development of a series of EGFR inhibitors against EGFR$^{19D/T790M/C797S}$ mutation based on Osimertinib (AZD9291) and compound **7** in Figure 2 reported with single-digit nanomolar $IC_{50}$ values against EGFR$^{L858R/T790M/C797S}$ mutation[18], some compounds displayed significant inhibitory activity against EGFR$^{19D/T790M/C797S}$ and good selectivity over EGFR WT, L858R/T790M and L858R/T790M/C797S respectively.

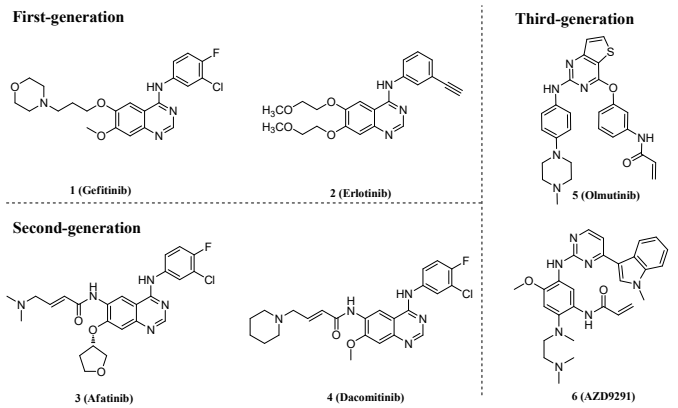


**Figure 1**. Structures of representative first-, second-, and third-generation EGFR inhibitors

inhibitors compound **7** and AZD9291 in Figure 2A, we found that two molecules exhibited similar binding modes. However, the additional hydrogen bond of compound **7** with the Asp855 side chain of the DFG motif stabilizes the flexible linker chain into an orientation directed away from Cys797, so we inferred that the alkyl chain terminal hydroxyl group of compound **7** extending to kinase phosphate binding site played a key role for the tertiary mutation inhibitory activity through a polar contact (H-O polar bond) with the Asp855 side chain in DFG motif. Therefore, with the help of molecular docking, the alkyl chain with terminal hydroxyl structural unit was introduced into the AZD9291 scaffold to increase interaction with the Asp855. So a series of indole derivatives were designed and prepared.

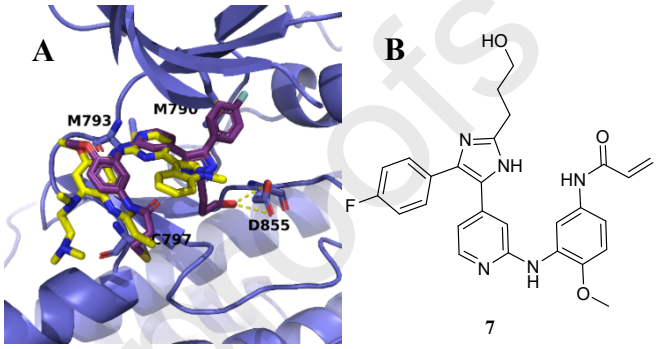


**Figure 2.** (A) Overlay poses between AZD9291 (yellow sticks, co complexed crystal conformation, PDB 4ZAU) and compound **7** docked with EGFR T790M (purple sticks, PDB 2JIU); (B) the structure of compound **7**.

Compound **8-12** were synthesized starting from *1H*-indole derivatives as presented in Scheme 1. A commercially available

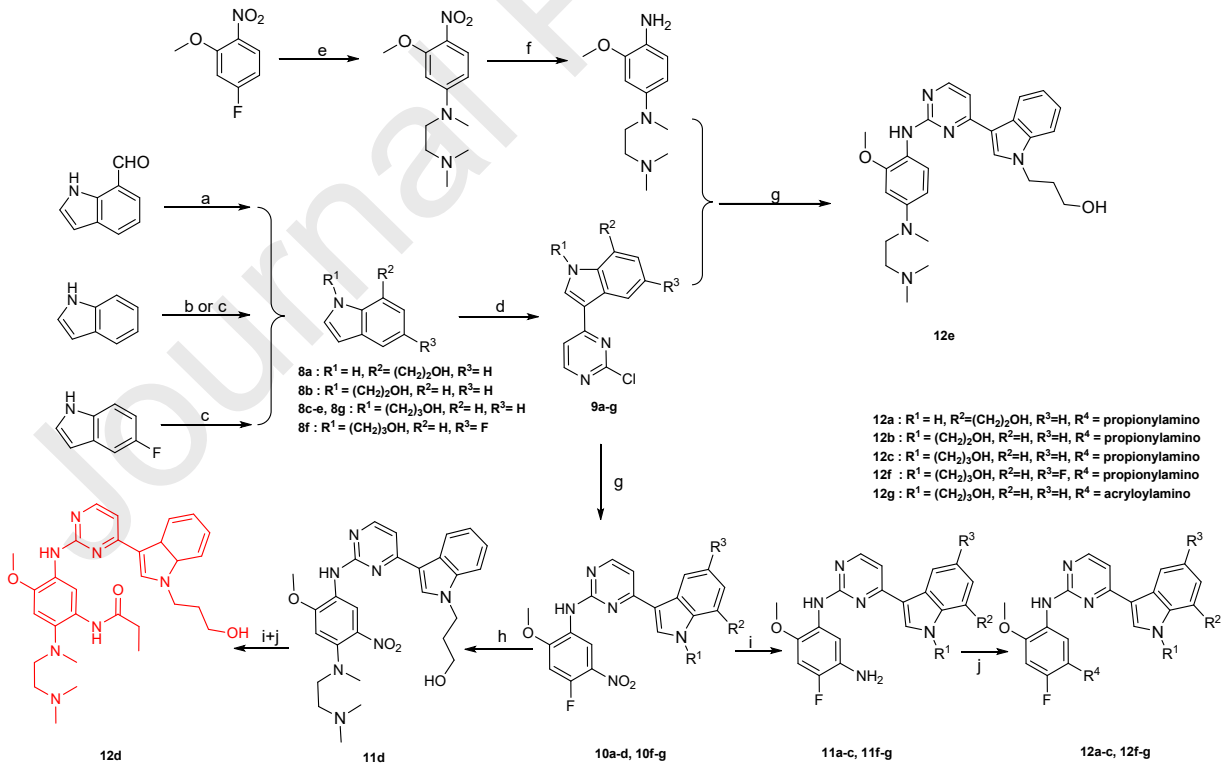


**Scheme 1**. [a]Reagents and conditions: (a) (1)$P(Ph)_3CH_2I$, KHMDS, THF, 25 °C, 2h, (2) $BH_3$ • THF, 0 °C, NaOH, $H_2O_2$, reflux, 1h; (b) (1) (2-bromoethanoxy)(tert-butyl)dimethylsilane, DMF, NaH, 100 °C, 4h;, (2) TBAF, THF, 25 °C, 4h; (c) DMSO, KOH, 25 °C, 8 h; (d) (1) DCE, anhydrous $AlCl_3$, 0 °C, (2) 2,4-dichloropyrimidine, 55 °C, 1.5 h; (e) *N,N,N'*- trimethylethane -1,2-diamine , DMF, $K_2CO_3$, 110 °C, 3 h; (f) 10%Pd/C, $H_2$, MeOH, 25 °C, 5 h; (g)

TsOH, DCM, AcOH, 55 °C, 4 h; (j) acryloyl chloride, DCM, DIPEA, 0 °C, 1.5 h.

*1H*-indole derivatives were carried out with Friedel-Crafts alkylation reaction after 2,4-dichloropyrimidine addition to afford compound **9a-g**. Subsequently, compound **10a-d&10f-g** were synthesized by the nucleophilic substitution of **9a-d&f-g** with 4-fluoro-2-methoxy-5-nitroaniline. The nitro group of compound **10a-d&10f-g** was performed reduction catalyzed by Fe powder in glacial acetic acid condition to yield corresponding amine, which was used in the next step without further purification. Finally, the target compounds **12a-d&f-g** were prepared by an acylation reaction with either acryloyl chloride or propionyl chloride. Compound **12e** was also synthesized by the nucleophilic substitution of **9e** with $N^1$-(2-(dimethylamino)ethyl)-3-methoxy-$N^1$-methylbenzene-1,4-diamine.

Considering the possibility for polar interactions with Asp855 in phosphate-binding site, we first obtained compounds bearing the hydroxyethyl group in different positions at the indole moiety. **12b** ($IC_{50}$ = 80.5 nM) with hydroxyethyl in $R^1$-postion showed better inhibitory activity against $EGFR^{19D/T790M/C797S}$ mutation than **12a** ($IC_{50}$ = 663.4 nM) with hydroxyethyl in $R^2$-postion. Then, we tested the effects of length of the terminal hydroxyl alkyl group on inhibitory activity. **12c** ($IC_{50}$ = 72.5 nM) with 1'-hydroxypropyl had slight advantage over 1'-hydroxyethyl **12b**.

In the solvent-exposed region, the binding mode in Figure 2A revealed that hydrophilic tail was oriented to solvent-exposed region. Therefore, we introduced a hydrophilic group ethylenediamine in an attempt to increase inhibitory activity. **12d** ($EGFR^{19D/T790M/C797S}$ $IC_{50}$ = 73.0 nM) displayed about same inhibitory activity comparable to **12c** ($IC_{50}$ = 72.5 nM), which suggested that the structure modification of solvent region had little effect on the molecular level activity.

Furthermore, in order to explore whether the substituent on indole benzene ring had any effects on the bioactivity, **12f** with F substitution in $R^3$-postion was synthesized. As a result, **12f** displayed similar bioactivities to that of **12c** in EGFR wild-type and mutations. For $EGFR^{19D/T790M/C797S}$ mutation, **12f** ($IC_{50}$ = 40.4 nM) showed 2 times more potent in contrast to **12c** ($IC_{50}$ = 72.5 nM), in fact the substitution effect on indole benzene ring was not obvious.

To our delighted, we obtained **12g** with a high inhibitory activity against $EGFR^{L858R/T790M}$ ($IC_{50}$ = 2.2 nM) and $EGFR^{19D/T790M/C797S}$ ($IC_{50}$ = 17.9 nM) and high selectivity over EGFR wild-type and $EGFR^{L858R/T790M/C797S}$ mutation. **12g** with Michael receptor on $R^4$-position represented typical third generation EGFR inhibitor. To verify the effects of substituents acrylamide, we could compare **12c** with propionamide on $R^2$-position **12g**, its inhibitory activity against $EGFR^{L858R/T790M}$ and $EGFR^{19D/T790M/C797S}$ was both weaker than **12g**, especially the inhibitory activity against $EGFR^{L858R/T790M}$ (2.2 nM vs 126.8 nM), which demonstrated that acrylamide was the key Michael receptor for a third generation EGFR inhibitor and not too critical for $EGFR^{19D/T790M/C797S}$.

To prove this inference above, compound **12e** (Figure S1) with $R^4$=H was obtained at last. The results were exactly as expected, **12e** showed the best inhibitory activity ($IC_{50}$ = 15.3 nM) against $EGFR^{19D/T790M/C797S}$ and excellent selectivity over EGFR wild-type and other mutations. We could conclude that **12e** was a promising fourth generation drug lead compound for $EGFR^{19D/T790M/C797S}$.

.

**Table 1**. Determination of Inhibitory Activities against EGFR Wild-Type (WT), L858R/T790M (LR/TM), L858R/T790M/C797S (LR/TM/CS) and 19D/T790M/C797S (19D/TM/CS)[a].

| Compound | | EGFR $IC_{50}$[nM] | | | |
|---|---|---|---|---|---|
| | | WT | LR/TM | LR/TM/CS | 19D/TM/CS |
| **12a** | 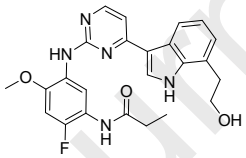 | > 1000 | 208.0 ± 16.2 | >1000 | 663.4 ± 154.5 |
| **12b** | 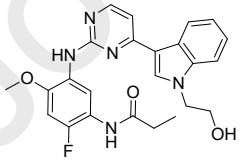 | > 1000 | 170.1 ± 9.5 | > 1000 | 80.5 ± 21.6 |
| **12c** | 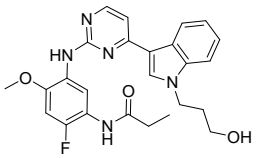 | > 1000 | 126.8 ± 10.5 | 422.3 ± 211.5 | 72.5 ± 2.4 |

| | | | | | |
|---|---|---|---|---|---|
| **12d** | 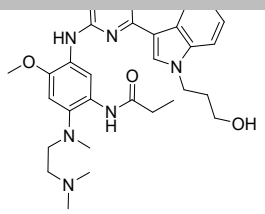 | > 1000 | 169.3 ± 16.5 | 638.4 ± 129.4 | 73.0 ± 14.9 |
| **12e** | 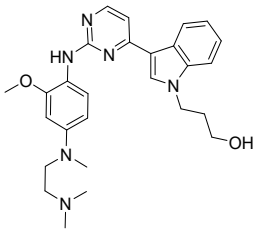 | > 1000 | 156.6 ± 2.8 | 218.3 ± 29.8 | 15.3 ± 1.4 |
| **12f** | 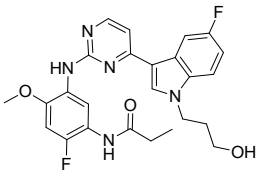 | > 1000 | 142.0 ± 3.1 | 332.2 ± 194.6 | 40.4 ± 4.5 |
| **12g** | 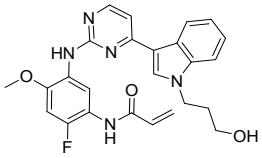 | 282.5 ± 54.5 | 2.2 ± 0.5 | >1000 | 17.9 ± 2.7 |
| **Brigatinib** | | 48.3 ± 8.7 | 1.5 ± 0.4 | 2.5 ± 0.2 | 1.5 ± 0.1 |
| **AZD9291** | | 332.6 ± 185.3 | 7.2 ± 3.3 | 167.1 ± 40.0 | / |

[a]Kinase activity assays were examined by using the ELISA-based EGFR-TK assay. Data are averages of at least two independent determinations and reported as the means ± SDs.

To further clarify the structure-activity relationship, molecular docking was adopted to explain the binding modes of compound **12a**, **12b** and **12c**. We inferred that the difference of the activities between **12a** and **12b** may be attributed to the fact that 1'-hydroxyethyl substitution could lead to a better orientation towards Asp855. Indeed, a polar contact (H-O polar bond) between the terminal hydroxyl group of **12b** with the Asp855 side chain could be seen, which could not be seen in 7'-hydroxyethyl **12a**. In addition, **12c** with 1'-hydroxypropyl formed an additional hydrogen bond with Lys745 led it to a slight advantage over 1'-hydroxyethyl **12b** (Figure 3A), thus **12c** showed the best activity among them.

Moreover, both 12c and 12g could form hydrogen bond interaction with Asp855 and Lys745 side chain through the terminal hydroxyl alkyl group. However, **12g** with Michael receptor on $R^2$-position formed a covalent bond with Cys797 (Figure 3B), which could explain its high inhibitory activity against $EGFR^{L858R/T790M}$ ($IC_{50}$ = 2.2 nM). Compared with **12g**, **12c** with propionamide on $R^2$-position could not form a covalent bond with Cys797 result in a weaker inhibitory activity against $EGFR^{L858R/T790M}$ ($IC_{50}$ = 126.8 nM), As for the tertiary EGFR exon 20 C797S mutation, a tertiary Cys797 to Ser797 point mutation disturbed the corresponding covalent bond formation, thus the activity difference between **12c** and **12g** was not as significant as that in $EGFR^{L858R/T790M}$, which demonstrated that acrylamide was the key Michael receptor for a third generation EGFR inhibitor and not too critical for $EGFR^{19D/T790M/C797S}$. Furthermore, the representative compound **12e** with $R^4$=H bound in ATP-binding cleft of the $EGFR^{T790M/C797S}$ mutants, maintaining the hydrogen bonds with Met793 by the structure of aminopyrimidine. Besides, the terminal hydroxyl group formed two hydrogen bonds with Asp855 and Lys745 respectively while the hydrophilic group ethylenediamine formed salt bridge interaction with Asp800 (Figure 3C). In brief, compared with solvent region and Michael receptor group, we thought that the introduction of the alkyl chain with terminal hydroxyl structural unit was considerable for the improvement of activity against 19D/TM/CS, which could explain the reason that the compounds **12g** with key Michael receptor still showed strong activities against 19D/TM/CS. That is, when an appropriate alkyl chain with terminal hydroxyl structural unit was added to the AZD9291 scaffold, the indole derivatives (such as **12e**) could form a

hydr… and enhance the inhibitory activity against EGFR$^{L858R/T790M/C797S}$, which coincided with our original design idea.

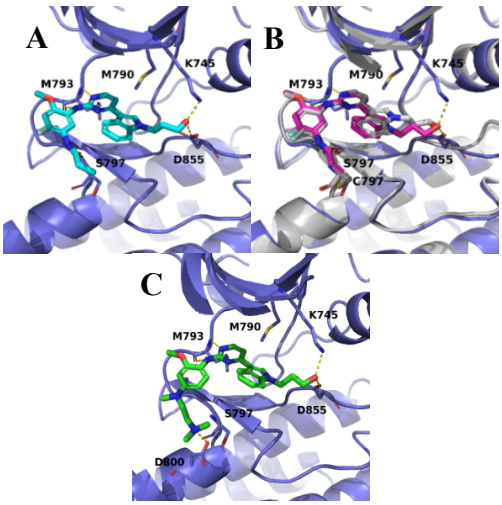


**Figure 3.** (A) The docked binding modes of **12c** in EGFR$^{T790M/C797S}$ mutant (blue sticks, PDB 5ZTO); (B) The overlaid docked binding modes of **12g** in EGFR$^{L858R/T790M}$ mutant (white sticks, PDB 5Y25) and EGFR$^{T790M/C797S}$ mutant (pink sticks, PDB 5ZTO) (C) The docked binding modes of **12e** in EGFR$^{T790M/C797S}$ mutant (green sticks, PDB 5ZTO).

The antiproliferative activities of **12e** were investigated against a panel of cancer cells including EGFR-overexpressing A431 and BaF3/EGFR$^{19D/T790M/C797S}$ cells. It was shown that **12e** potently inhibited the proliferation of BaF3 cells harboring the EGFR$^{19D/T790M/C797S}$ mutant with $IC_{50}$ value at 8.51 μM (Figure 4, Table 2) which was comparable with Brigatinib. **12e** also inhibited the growth of A431 and H1975 cells with an $IC_{50}$ values of 20.48 and 16.18 μM, respectively.

The mechanism of cell death was evaluated by two-dimensional cell sorting by staining DNA with PI and staining phosphatidylserine (PS) with a fluorescent annexin V derivative. We evaluated the effects of compound **12e** after 24 h treatments in BaF3/EGFR$^{19D/T790M/C797S}$ cells. As shown in Figure 5, compound **12e** induced apoptosis of BaF3/EGFR$^{19D/T790M/C797S}$ cells in a concentration-dependent manner. It induced 24.18% early-stage apoptosis and 14.53% late-stage apoptosis at 10 μM concentration, and 74.01% early-stage apoptosis and 23.81% late-stage apoptosis at 50 μM concentration. The percentage of apoptosis in the **12e**-treated group was higher than that in the control group.

**Table 2**. Antiproliferative Activities of **12e** against Cells with Different Mutant EGFR[a]

| Comp. | $IC_{50}$, μM. | | | A431 / H1975 | A431 / BaF3/EGFR$^{19D/TM/CS}$ |
|---|---|---|---|---|---|
| | A431 | H1975 | BaF3/EGFR$^{19D/TM/CS}$ | | |
| **12e** | 20.48 ± 1.15 | 16.18 ± 0.82 | 8.51 ± 0.78 | 1.27 | 2.41 |
| **Brigatinib** | 1.51 ± 0.35 | 0.74 ± 0.11 | 5.47 ± 0.56 | 2.04 | 0.28 |

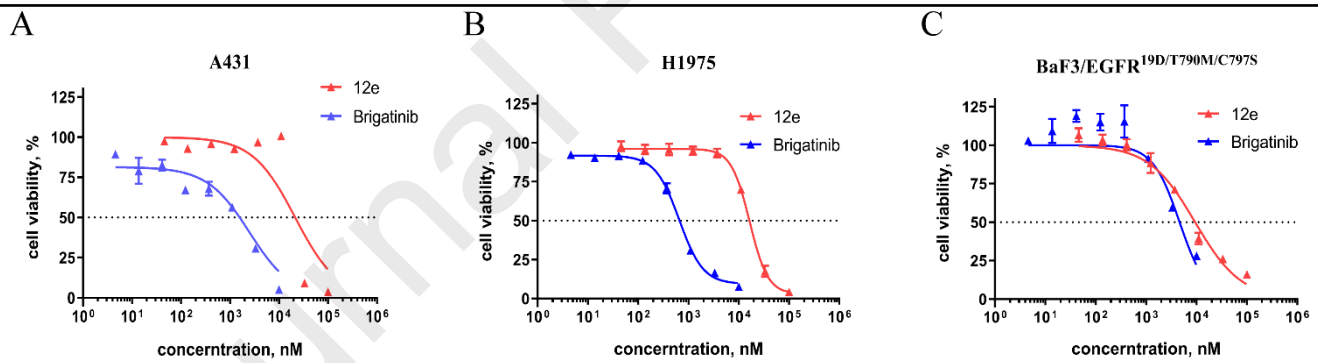


**Figure 4**. The in vitro cell inhibitory efficacy of **12e** against A431(A), H1975(B), and BaF3/EGFR$^{19D/T790M/C797S}$ (C) were tested by CCK-8 assay.

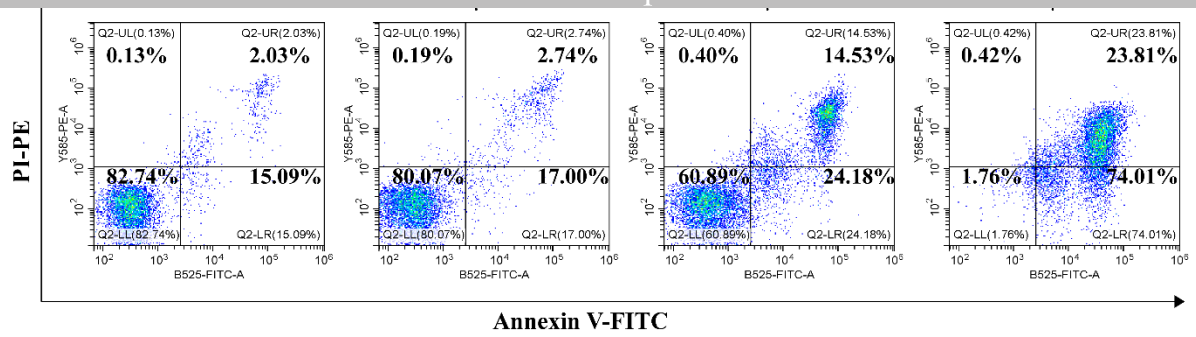


**Figure 5.** Apoptotic effect of **12e** on BaF3/EGFR$^{19D/T790M/C797S}$ cells after treatment for 24 h. The lower left quadrant represents live cells, the lower right is for early/primary apoptotic cells, the upper right is for late/secondary apoptotic cells, and the upper left represents cells damaged during the procedure.

To demonstrate the effect of compound **12e** on the cell cycle, we used flow cytometry for analysis. BaF3/EGFR$^{19D/T790M/C797S}$ cells were treated with compound **12e** (1, 10, and 20 μM) and brigatinib (1 μM). As shown in Figure 6A, the percentage of cells in the G1, S and G2 phase was obtained with flow cytometry, and then summarized in Figure 6B. Compound **12e** caused accumulation of cells in the G1 phase of the cell cycle in a dose-dependent manner. The percentage of G1 phase cells from 39.62% to 53.37% from absence to the presence of 20 μM **12e**.

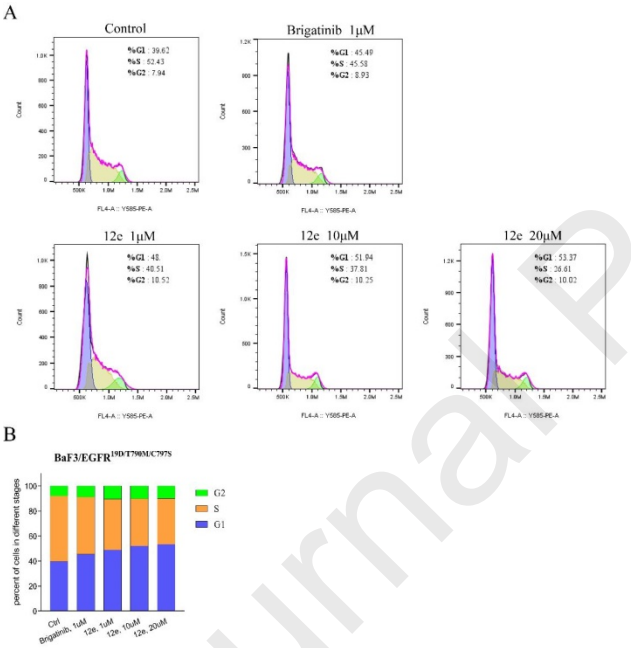


**Figure 6.** Effect of **12e** on cell cycle progression in BaF3/EGFR$^{19D/T790M/C797S}$ cells. (A) Cells were treated with different concentrations of **12e** and brigatinib for 24 h, then the cell cycle distribution was analyzed by flow cytometry. (B) Graph reporting percentile cell-cycle phase distributions. G1, S and G2 phase distributions were determined by FlowJo analysis.

We evaluated **12e** of its ability to interfere with EGFR and downstream signaling. To this end, BaF3/EGFR$^{19D/T790M/C797S}$ cells were treated with different doses of **12e** and analyzed the phosphorylation of EGFR and downstream molecules Akt and ERK. As shown in Figure 7, **12e** significantly induced reduction of phosphorylated EGFR and ERK in a dose-dependent manner, and phosphorylated Akt signal decreased slightly.

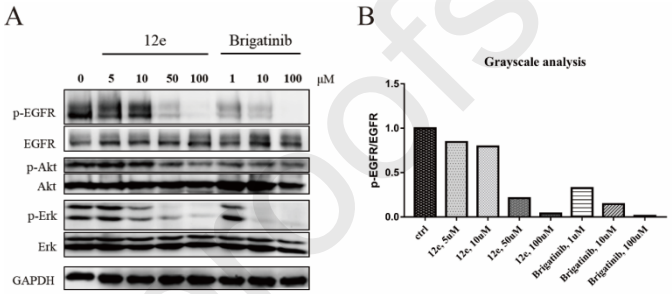


**Figure 7.** (A) BaF3 cells that overexpressed EGFR$^{19D/T790M/C797S}$ were treated with the indicated concentrations of **12e**, and brigatinib for 3 h and stimulated by EGF for 10 min. Cell lysates were harvested for Western blot analysis for EGFR, Akt and ERK phosphorylation. (B) Protein bands were quantified using ImageJ and GraphPad Prism software.

In conclusion, to overcome this resistance mutation 19D/T790M/C797S, a series of indole derivatives bearing alkyl chains with the terminal hydroxyl group which formed the hydrogen bond with Asp855 and intended to increase the binding affinities of the AZD9291 were synthesized and evaluated as potent EGFR$^{19D/T790M/C797S}$ inhibitors. The results were exactly as expected through structure-activity relationship and docking analysis. The representative compound **12e** strongly inhibited the kinase activity of EGFR$^{19D/T790M/C797S}$ with $IC_{50}$ value of 15.3 nM and exhibited highly selectivity over EGFR$^{WT}$ and EGFR$^{L858R/T790M/C797S}$. Meanwhile, **12e** could significantly suppress the EGFR phosphorylation and its downstream signaling molecules Akt and ERK, induce the apoptosis, arrest cell cycle at G1, and inhibit proliferation with $IC_{50}$ values of 8.5 μM in BaF3/EGFR$^{19D/T790M/C797S}$ cells in a concentration-dependent manner. Our study provided a novel structural design concept which is promising for the development of the fourth-generation EGFR$^{19D/T790M/C797S}$ inhibitors.

## Acknowledgments

The research is supported in part by the National Key Research and Development Program (Grant 2016YFA0502304), the National Natural Science Foundation of China (grant 81825020), the National Science & Technology Major Project "Key New Drug Creation and Manufacturing Program", China (No. 2018ZX09711002), the Special Program for Applied Research on Super Computation of the NSFC-Guangdong Joint Fund (the second phase) under Grant No. U1501501. Honglin Li is also sponsored by National Program for Special Supports of Eminent Professionals and National Program for Support of Top-Notch Young Professionals.

1. Bray, F.; Ferlay, J.; Soerjomataram, I.; Siegel, R. L.; Torre, L. A.; Jemal, A. *CA: a cancer journal for clinicians* **2018,** *68*, 394.
2. Appert-Collin, A.; Hubert, P.; Cremel, G.; Bennasroune, A. *Frontiers in pharmacology* **2015,** *6*, 283.
3. Cohen, M. H.; Williams, G. A.; Rajeshwari, S.; Gang, C.; W David, M.; David, M.; Sophia, A.; Atiqur, R.; Chenyi, L.; Richard, L. *Clinical Cancer Research An Official Journal of the American Association for Cancer Research* **2004,** *10*, 1212.
4. Xu, Y.; Liu, H.; Chen, J.; Zhou, Q. *Cancer biology & therapy* **2010,** *9*, 572.
5. Bean, J.; Riely, G. J.; Balak, M.; Marks, J. L.; Ladanyi, M.; Miller, V. A.; Pao, W. *Clinical cancer research : an official journal of the American Association for Cancer Research* **2008,** *14*, 7519.
6. Singh, M.; Jadhav, H. R. *Drug discovery today* **2018,** *23*, 745.
7. Specenier, P.; Vermorken, J. *Expert opinion on pharmacotherapy* **2016,** *17*, 1295.
8. Soria, J. C.; Sequist, L. V.; Gadgeel, S.; Goldman, J.; Wakelee, H.; Varga, A.; Fidias, P.; Wozniak, A. J.; Neal, J. W.; Doebele, R. C. *Journal of Thoracic Oncology* **2014,** *32*, S141.
9. Jiang, T.; Zhou, C. *Translational Lung Cancer Research* **2014,** *3*, 370.
10. Thress, K. S.; Paweletz, C. P.; Felip, E.; Cho, B. C.; Stetson, D.; Dougherty, B.; Lai, Z.; Markovets, A.; Vivancos, A.; Kuang, Y.; Ercan, D.; Matthews, S. E.; Cantarini, M.; Barrett, J. C.; Janne, P. A.; Oxnard, G. R. *Nature medicine* **2015,** *21*, 560.
11. Song, H. N.; Jung, K. S.; Yoo, K. H.; Cho, J.; Lee, J. Y.; Lim, S. H.; Kim, H. S.; Sun, J. M.; Lee, S. H.; Ahn, J. S.; Park, K.; Choi, Y. L.; Park, W.; Ahn, M. J. *Journal of thoracic oncology : official publication of the International Association for the Study of Lung Cancer* **2016,** *11*, e45.
12. Chabon, J. J.; Simmons, A. D.; Lovejoy, A. F.; Esfahani, M. S.; Newman, A. M.; Haringsma, H. J.; Kurtz, D. M.; Stehr, H.; Scherer, F.; Karlovich, C. A.; Harding, T. C.; Durkin, K. A.; Otterson, G. A.; Thomas Purcell, W.; Ross Camidge, D.; Goldman, J. W.; Sequist, L. V.; Piotrowska, Z.; Wakelee, H. A.; Neal, J. W.; Alizadeh, A. A.; Diehn, M. *Nature communications* **2016,** *7*, 13513.
13. Grabe, T.; Lategahn, J.; Rauh, D. *ACS medicinal chemistry letters* **2018,** *9*, 779.
14. Park, H.; Jung, H. Y.; Mah, S.; Hong, S. *Angewandte Chemie* **2017,** *56*, 7634.
15. Gunther, M.; Lategahn, J.; Juchum, M.; Doring, E.; Keul, M.; Engel, J.; Tumbrink, H. L.; Rauh, D.; Laufer, S. *J Med Chem* **2017,** *60*, 5613.
16. Li, Q.; Zhang, T.; Li, S.; Tong, L.; Li, J.; Su, Z.; Feng, F.; Sun, D.; Tong, Y.; Wang, X.; Zhao, Z.; Zhu, L.; Ding, J.; Li, H.; Xie, H.; Xu, Y. *ACS medicinal chemistry letters* **2019,** *10*, 869.
17. Wang, S.; Tsui, S. T.; Liu, C.; Song, Y.; Liu, D. *Journal of hematology & oncology* **2016,** *9*, 59.
18. Chen, L.; Fu, W.; Zheng, L.; Liu, Z.; Liang, G. *J Med Chem* **2017,** *60*, 5613.


**Supplementary Material**

Supplementary material that may be helpful in the review process should be prepared and provided as a separate electronic file. That file can then be transformed into PDF format and submitted along with the manuscript and graphic files to the appropriate editorial office.

## Declaration of interests

☒ The authors declare that they have no known competing financial interests or personal relationships that could have appeared to influence the work reported in this paper.

☐The authors declare the following financial interests/personal relationships which may be considered as potential competing interests: